PHYSICAL REVIEW E **68**, 056404 (2003)

Electric and magnetic field generation and target heating by laser-generated fast electrons

J. R. Davies*
GoLP, Instituto Superior Técnico, 1049-001 Lisboa, Portugal
(Received 5 May 2003; published 20 November 2003)

The electric and magnetic fields generated by a beam of fast electrons in a conductor are calculated analytically, including the change in resistivity due to Ohmic heating. It is assumed that the resistivity has an arbitrary power law dependence on temperature, the fast electron current density is fixed (rigid beam), charge neutralization is instantaneous, and that magnetic diffusion is negligible. The implications for high-intensity laser-solid interactions are discussed. The minimum fast electron density for fast ignition by Ohmic heating is given, and found to be unrealistically high.

DOI: 10.1103/PhysRevE.68.056404 PACS number(s): 52.38.−r, 52.57.Kk

I. INTRODUCTION

Experiments on high-intensity laser interactions with solid targets have renewed interest in the transport of high-current electron beams in conductors, as a significant fraction of the laser energy can be transferred into high-energy, or fast, electrons entering the target. An application of such laser-generated electron beams, which has received a lot of attention, is the fast ignitor [1]. In this scheme, it is proposed to use the electrons to rapidly heat the core of a compressed fuel pellet to ignition, before pressure balance is reached. This would achieve higher gain than the slower, conventional method of driving shocks into the target. A large amount of work has been carried out on the transport of high-current electron beams in conductors (which includes most materials at the currents we are interested in) outside the context of laser plasmas [2]. Interestingly, igniting a plasma with an electron beam was one of the applications considered. The transport of such beams is strongly affected by the fields that they generate. The field generation is dependent on the conductor's ability to cancel the beam's charge and current density. The simplest model for the response of the conductor is the basic Ohm's law

$$\mathbf{E}=\eta\mathbf{j}_c, \tag{1}$$

where $\mathbf{E}$ is the electric field, $\mathbf{j}_c$ is the current density in the conductor, and η is its resistivity. This model has been used extensively in calculations of electron beam transport. For simple cases analytic solutions can be found.

Bell *et al.* [3] obtained self-similar solutions for the propagation of a Maxwellian distribution of fast electrons into a semi-infinite target, with a constant resistivity, in one dimension. For a total number of fast electrons growing linearly in time Bell *et al.* obtained a mean penetration depth

$$L=\frac{4\langle K\rangle}{3e\,\eta j_0}, \tag{2}$$

where $\langle K\rangle$ is the mean fast electron energy and j_0 is the current density of the fast electron source. This is roughly the distance an electron with the mean energy would travel against the initial electric field ηj_0. Davies [4] has considered this model for various Maxwellian distributions (Bell *et al.* used a three-component, nonrelativistic Maxwellian). Batani *et al.* [5] have considered the scaling of this penetration depth with target density for the Spitzer resistivity and strong target heating. We will return to this later. Glinsky [6] considered a more complete one-dimensional model, using the Spitzer resistivity, including fast electron collisions and heat flow. However, he was only able to estimate temporal regimes in which different terms would dominate, and give scalings for the essential parameters in these regimes.

Analytic solutions can be found for certain equilibria [2]. However, these are of limited application in the study of the dynamics of propagating beams.

A further assumption that greatly simplifies calculations is to assume a fixed fast electron current density. This is often referred to as the rigid beam model. Clearly this does not model the dynamics of the beam, but rather the response of the conductor to a given fast electron current density. It will only be valid while the fast electrons remain strongly relativistic and the magnetic field is negligible. However, it allows analytic solutions to be obtained, which are useful in understanding more complex models, in identifying important effects, and in making crude estimates. The objective here is to use this model to evaluate the effect of the changes in resistivity caused by Ohmic heating on the field generation. For current densities given by certain special functions it is possible to solve the full Maxwell's equations for a constant resistivity [2]. The details of these results are not of interest here, but they establish two important time scales: the neutralization time (τ_n) and the magnetic diffusion time (τ_d). Charge and current neutralization of the beam are established over a time scale

$$\tau_n=\varepsilon_0\eta, \tag{3}$$

which is extremely rapid; for a resistivity of 2 $\mu\Omega$ m, a typical upper limit for solid density conductors [7,8], it is only 17.7 as (atto$=10^{-18}$). In using Eq. (1) we are ignoring processes occurring on time scales less than the plasma period of the conductor, which is often greater than this neutralization time. Although rapid, beam neutralization is not instantaneous, and therefore it is not exact, leading to field genera-

*Electronic address: jdavies@popsrv.ist.utl.pt

tion. The transverse separation of the currents leads to the generation of a magnetic field, which acts to further separate the currents (opposite currents repel). The return current decays on a time scale given by the magnetic diffusion time

$$\tau_d = \frac{\mu_0 R^2}{\eta}, \tag{4}$$

where R is the transverse scale length of the fast electron beam. This is a relatively slow process; for a transverse scale length of 10 μm and a resistivity of 2 $\mu\Omega$ m the magnetic diffusion time is 62.8 ps, much longer than the typical pulse durations of high-intensity lasers, and the maximum pulse duration predicted for the fast ignitor scheme [1]. This means that for most cases of interest we can greatly simplify the equations, neglecting the displacement current (which provides the initial current neutralization) and assuming $\mathbf{j}_c \approx -\mathbf{j}$. The electric and magnetic fields are then given by

$$\mathbf{E} \approx -\eta \mathbf{j}, \tag{5}$$

$$\frac{\partial \mathbf{B}}{\partial t} \approx \nabla \times \eta \mathbf{j}. \tag{6}$$

The model is quasineutral in both charge density and current density. The total charge and current densities are assumed to be much smaller than those of the fast electrons, and are not considered explicitly. The equations for $\nabla \cdot \mathbf{E}$ and $\nabla \times \mathbf{B}$ can be used to calculate the total charge and current densities, respectively, to check the validity of the quasineutral assumption, but they are not used in the calculation of the fields. This may appear counterintuitive at first, as the charge and current densities are the sources of the fields, however, when we take into account that the total values are determined by very small differences between two large quantities, we see that such an approach would be strongly prone to error. The assumptions used in obtaining these results are (i) all time scales are much greater than τ_n [Eq. (3)] and the plasma period of the conductor, and much less than τ_d [Eq. (4)]; (ii) all spatial scales are much greater than $c\tau_n$ and the skin depth of the conductor, and (iii) the collisional drag on the conduction electrons is much greater than the forces from the magnetic field and the pressure gradient. These assumptions are satisfied if the fast electron density is much less than that of the conductor, and for times much less than τ_d. This approximation has been used to evaluate field generation in laser-solid interactions for a constant resistivity by a number of authors [9–11]. Here we extend these calculations to include a resistivity of the form

$$\eta = \eta_0 \left(\frac{T}{T_0} \right)^{\alpha}, \tag{7}$$

where the subscript 0 indicates initial values and α is an arbitrary constant. To calculate the temperature we consider just Ohmic heating and neglect thermal conduction, giving

$$\frac{\partial T}{\partial t} = \frac{\eta j^2}{C}, \tag{8}$$

where C is the heat capacity term, assumed to be constant. We write it in terms of the electron density of the conductor n_c as

$$C = f k n_c, \tag{9}$$

where f is a dimensionless constant and k is Boltzmann's constant. We will now solve these equations, and then discuss the implications of the results for laser-solid interactions, making comparisons with the results of numerical modeling [7,9,12–14], and estimate the beam parameters required for fast ignition by Ohmic heating.

II. RESULTS

To simplify calculation, we assume rotational symmetry and consider a fast electron current density with only an axial component ($\boldsymbol{j} = j\hat{\boldsymbol{z}}$). The electric field is then predominantly axial ($\boldsymbol{E} = E\hat{\boldsymbol{z}}$) and the magnetic field azimuthal ($\boldsymbol{B} = B\hat{\boldsymbol{\theta}}$). Although it is possible to solve the equations for, almost, arbitrary current densities, it does not detract from our understanding of the essential physics to simply consider a blunt beam, moving at speed v along the axis, with a current density that varies only with radius. With these assumptions, all quantities can be represented as scalars that are functions of only radius r and the time variable

$$\tau \equiv t - \frac{z}{v} \geqslant 0, \tag{10}$$

which gives the length of time that the beam has been passing a given point. We assume that the beam is generated from $z=0$ starting at $t=0$, thus $\tau=0$ is the beam front and $\tau=t$ is the source of the beam. We will take the maximum value of τ to be given by the laser pulse duration. The equations are not actually valid at the front of a blunt beam, as the current density clearly changes over a distance less than either $c\tau_n$ [Eq. (3)] or the skin depth. There will be a nonneutral sheath region around the front of the beam [2], but this will affect only a very small region.

Substituting Eq. (7) into Eq. (8) gives a first-order differential equation for the temperature, which has two different solutions depending on the value of α. We have

$$T = T_0 \left(1 + (1-\alpha) \frac{\eta_0 j^2 \tau}{C T_0} \right)^{1/(1-\alpha)}, \quad \alpha < 1. \tag{11}$$

Although this is also valid for $\alpha > 1$, the temperature then goes infinite at $\tau = C T_0 / (\alpha - 1) \eta_0 j^2$. As we do not encounter materials with resistivities growing faster than linearly with temperature, this is not a problem. The other solution is

$$T = T_0 \exp\left(\frac{\eta_0 j^2 \tau}{C T_0} \right), \quad \alpha = 1. \tag{12}$$

The electric field [Eq. (5)] is then

$$E = -\eta_0 \left(1 + (1-\alpha) \frac{\eta_0 j^2 \tau}{C T_0} \right)^{\alpha/(1-\alpha)} j, \quad \alpha < 1, \tag{13}$$

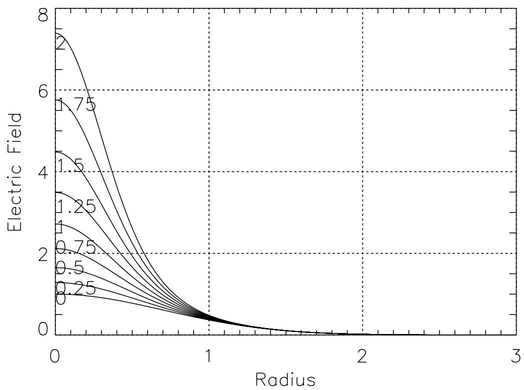

FIG. 1. The electric field for $\alpha=1$ and the current density given by Eq. (17) for the indicated values of τ. Normalized units explained in the text.

$$E=-\eta_0 \exp\left(\frac{\eta_0 j^2 \tau}{CT_0}\right) j, \quad \alpha=1. \tag{14}$$

The magnetic field is given by integrating Eq. (6) with respect to τ. Making use of a change of variable to T, we obtain

$$B=-\frac{dj}{dr}\frac{CT_0}{j^2}\left(1+\frac{1+\alpha}{1-\alpha}\frac{T}{T_0}-\frac{2}{1-\alpha}\frac{\eta}{\eta_0}\right), \quad \alpha<1, \tag{15}$$

$$B=-\frac{dj}{dr}\frac{CT_0}{j^2}\left[1+\left(\frac{2\eta_0 j^2\tau}{CT_0}-1\right)\frac{T}{T_0}\right], \quad \alpha=1. \tag{16}$$

This completes the solution.

III. DISCUSSION

To illustrate our discussion we will use a current density

$$j=-j_0 \exp\left(-\frac{r^2}{R^2}\right), \tag{17}$$

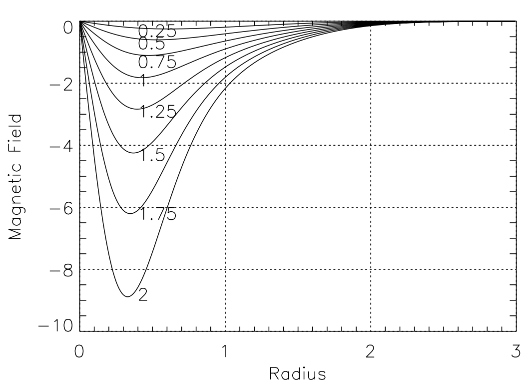

FIG. 2. The magnetic field for $\alpha=1$ and the current density given by Eq. (17) for the indicated values of τ. Normalized units explained in the text.

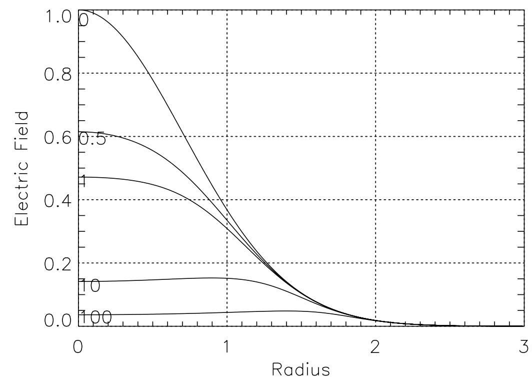

FIG. 3. The electric field for $\alpha=-3/2$ and the current density given by Eq. (17) for the indicated values of τ. Normalized units explained in the text.

chosen for its mathematical simplicity (the exact form is not important) and because laser intensities typically fall with radius (the minus sign is to make j_0 positive for electrons flowing in the positive z direction), and values of α of 1 and $-3/2$, chosen to represent two possible extremes. The electric and magnetic fields for these cases are given in Figs. 1–4. Current density has been normalized to j_0, resistivity to η_0, temperature to T_0 and distance to R. This gives electric field in units of $\eta_0 j_0$, magnetic field in units of CT_0/j_0R, and time in units of $CT_0/\eta_0 j_0^2$.

It is instructive to consider two limits of Eqs. (13)–(16): (i) $\eta_0 j^2\tau/CT_0 \ll 1$ and (ii) $\eta_0 j^2\tau/CT_0 \gg 1$. This parameter is the temperature increase caused while the resistivity equals its initial value, divided by the initial temperature. Therefore limit (i) corresponds to weak heating and limit (ii) to strong heating.

For weak heating we obtain, to first order in the heating parameter $\eta_0 j^2\tau/CT_0$,

$$E\approx-\eta_0\left(1+\alpha\frac{\eta_0 j^2\tau}{CT_0}\right)j, \tag{18}$$

$$B\approx-\eta_0\frac{dj}{dr}\tau, \tag{19}$$

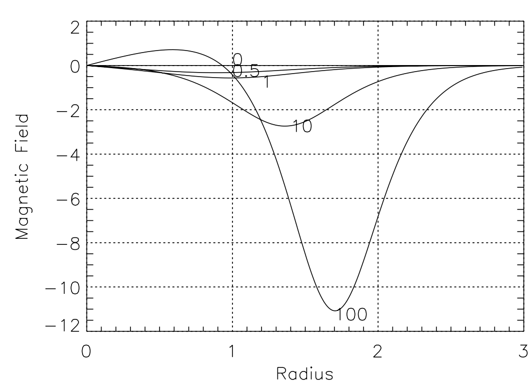

FIG. 4. The magnetic field for $\alpha=-3/2$ and the current density given by Eq. (17) for the indicated values of τ. Normalized units explained in the text.

whatever the value of α. These results apply near the front of the beam and at large radii. In this limit, only the electric field is affected by the heating, increasing or decreasing with time, or, equivalently, distance from the beam front, depending on whether the resistivity increases or decreases with temperature. One effect of this would be to make the mean penetration depth [Eq. (2)] dependent on the laser pulse duration. Glinsky [6] found that the fast electron penetration depth increased linearly in time at early times, as would be expected from Eqs. (2) and (18) for a negative value of α. The radial profile of the electric field is also changed, due to the j^2 dependence of the heating, increasing more rapidly with current density if the resistivity increases with temperature, and more slowly if it decreases. This can be seen in Figs. 1 and 3. As noted by Bell *et al.* [3], the increase in electric field with current density will act to reduce the penetration depth on axis. This would lead to the beam front becoming hollow. When the resistivity increases with temperature this will become more pronounced behind the beam front, which is not affected by the increase in resistivity. When the resistivity decreases with temperature this effect will be counteracted, as the beam front will be overtaken by the following electrons, which see a lower electric field that varies more slowly with current density. It will also be counteracted if the mean electron energy increases with the current density. As we expect both parameters to depend on the laser intensity, this may well be the case. This was assumed in our numerical modeling, where this hollowing of the beam front was found to be a weak, transitory effect [9]. The magnetic field [Eq. (19)] is zero at the beam front and initially grows linearly with time. This can be seen in Figs. 2 and 4. This time dependence of the magnetic field means that the fast electron transport will be strongly affected by the laser pulse duration. If the pulse duration is long enough [9], the magnetic field at the edge of the beam will eventually dominate over the electric field ($cB>E$), whatever the temperature dependence of the resistivity, as can be seen by comparing Figs. 1 and 2, and Figs. 3 and 4. The minus sign in Eq. (19) means that it acts to pinch the beam or to filament it if the current profile is irregular. Once this occurs, the current density will increase rapidly, and so will the electric and magnetic fields. This has been seen in our numerical modeling [9], where we found that the maximum fields obtained in runs with a fixed resistivity rapidly exceeded the rigid beam calculations due to the pinch effect, the difference being far greater for the magnetic field. Filamentation has been studied by Gremillet *et al.* [15]. This increase in current density will also lead to a more rapid transition to the strong heating regime.

For strong heating we obtain

$$E \approx -\eta_0^{1/(1-\alpha)} \left(\frac{(1-\alpha)\tau}{CT_0} \right)^{\alpha/(1-\alpha)} j^{(1+\alpha)/(1-\alpha)}, \quad \alpha<1, \tag{20}$$

$$E = \eta_0 \exp\left(\frac{\eta_0 j^2 \tau}{CT_0} \right) j, \quad \alpha=1, \tag{21}$$

$$B \approx -(1+\alpha)\eta \frac{dj}{dr}\tau, \quad \alpha \leqslant 1. \tag{22}$$

These results will apply some distance back from the beam front at small radii, provided that the pulse duration is long enough. We can identify three different regimes of behavior depending on the value of α; (i) $\alpha>0$, (ii) $-1<\alpha<0$, and (iii) $\alpha\leqslant-1$. In regime (i) the electric and magnetic fields increase more rapidly with both time and current density (Figs. 1 and 2). In regime (ii) the electric field falls in time and increases more slowly with current density, and the magnetic field increases more slowly with both time and current density. In regime (iii) both the electric and magnetic fields fall in time and no longer increase with current density. For $\alpha<-1$ the electric field decreases with current density, and the magnetic field changes sign (Figs. 3 and 4). For $\alpha=-1$ the electric field becomes independent of the current density and the magnetic field falls to zero. In all of the strong heating regimes, the effect of target heating is most notable in the magnetic field, on the contrary to the weak heating result. As can be seen from Eq. (22), in regime (i) the magnetic field is a factor of $(1+\alpha)$ higher than if the resistivity had maintained its maximum value throughout, in regime (ii) it is a factor of $(1+\alpha)$ lower than if the resistivity had maintained its minimum value throughout, and in regime (iii) the magnetic field either vanishes or reverses. A simple physical explanation for this is that the return current concentrates where the resistivity is lower, which is outside the beam when the resistivity increases with temperature and inside the beam when it decreases. The effect on the electric field is not as pronounced, as no matter where the return current flows the energy to drive it has to come from the fast electrons.

We will now consider the implications of these results for laser-solid interactions. Regime (i) applies to metals at low temperatures. For example, Milchberg *et al.* [8] found that the resistivity of aluminum increased up to a temperature (kT/e) of around 50 eV, before eventually decreasing, obeying the Sptizer resistivity ($\alpha=-3/2$) at high temperatures. This means that the fields in metals will be considerably higher than would be expected from their initially low resistivities. In particular, much higher magnetic fields could be generated in metals than in insulators, as can be seen by comparing Figs. 2 and 4, and this has been seen in numerical modeling [12]. As the magnetic field remains in the target, it will be important even if a metal is rapidly heated to temperatures where the resistivity starts to fall. This means that it is important to correctly model this low temperature behavior. This has been seen in our numerical modeling [9], where a large negative magnetic field remained near the source of the electron beam, even though temperatures high enough for the Spitzer resistivity to apply were reached.

Regime (ii) applies in metals during the transition from the peak resistivity to the Spitzer resistivity, and may apply in other cases, but is not of particular interest.

Regime (iii) will apply to all materials if the heating is strong enough, because at high enough temperatures the Spitzer resistivity ($\alpha=-3/2$) applies to all materials. This means that the result of truly strong target heating will be to lower the fields, and eventually to change the sign of the magnetic field. We can determine the heating parameter required for the electric field to fall with current density, and for the magnetic field generation to change sign, to be

$$-(1+\alpha)\frac{\eta_0 j^2 \tau}{CT_0}>1, \quad \alpha<-1. \tag{23}$$

We cannot, in general, solve the condition for the magnetic field to be positive, at which point the strong heating results should apply. We are interested in evaluating Eq. (23) for the Spitzer resistivity in laser-solid interactions. To do this, we assume that the heat capacity is that of an ideal gas at constant volume [Eq. (9) with $f=3/2$] and write the current density as $ef_{abs}I/\langle K\rangle$, where I is the laser intensity and f_{abs} is the absorption into fast electrons, and take the mean fast electron energy to be given by the ponderomotive potential for $I\lambda^2 \gg 10^{10}$ W, where λ is the laser wavelength, which is $\langle K\rangle/e \approx 4.77(I\lambda^2)^{1/2}$ eV. This gives

$$4.25\times 10^{19}\frac{\eta_0^{5/3} f_{abs}^2 I\tau}{Z^{5/3} n_a (\ln\Lambda)^{2/3}\lambda^2}>1, \tag{24}$$

where Z is atomic number, $\ln\Lambda$ comes from the Spitzer resistivity, and we have used $n_c = Zn_a$, n_a being the atom number density, which varies little among solids. Solving the condition for the magnetic field to become positive numerically, shows that the heating parameter must be approximately 12 times higher than that given by Eq. (24). As an example, we use Eq. (24) to give a condition on the laser intensity for an aluminum target, an absorption of 30%, a laser pulse duration of 1 ps, and a wavelength of 1 μm, parameters used in much of the numerical modeling and relevant to many experiments. For the initial resistivity we use the measured maximum value [8] of ≈ 2 $\mu\Omega$ m, assuming that the heating up to this point is much faster, and we take $\ln\Lambda$ to be 10. From this we find that the intensity must be greater than 1.6×10^{22} W m^{-2} for the electric field to start to fall, and greater than 2.0×10^{23} W m^{-2} for the magnetic field to change sign. These values should be taken as estimates for the average intensities at which these effects will start to become important. We can also give the scaling of the fields with the laser parameters for the Spitzer resistivity in the strong heating regime

$$E \propto f_{abs}^{-1/5} I^{-1/10} \lambda^{1/5} t^{-3/5}, \tag{25}$$

$$B \propto f_{abs}^{-1/5} I^{-1/10} \lambda^{1/5} t^{2/5} R^{-1}. \tag{26}$$

From which we see that the fields will start to fall with increasing intensity, but very slowly, giving an effective saturation in the field generation with intensity. Saturation of the peak, negative, magnetic field has been observed in numerical modeling at a peak intensity of 5×10^{23} W m^{-2}, which is consistent with the above intensity estimates. The strongest scaling is with time, the electric field decreasing in time and the magnetic field increasing, but with the opposite sign to that generated initially. This again shows that fast electron transport will be strongly affected by pulse duration. The reversal of the magnetic field is the most significant change in the field generation for this regime. It will act to expand and hollow the beam. The generation of a positive magnetic field can be seen in Fig. 4. It starts near the axis and moves outwards, as the current density [Eq. (17)] is highest on axis. One can easily envisage the beam turning into an expanding annulus, being pushed outwards from the center and pinched inwards at the edge. Another point to note from Fig. 4 is that the negative peak in magnetic field continues to increase. When the resistivity falls linearly or faster with temperature the magnetic field is maximized for a low current density maintained for a long time, which translates to low laser intensities and long pulse durations. However, the increase in magnetic field with pulse duration will eventually be limited by magnetic diffusion. A falling magnetic field and the generation of a positive magnetic field near the axis has been consistently observed in all of our numerical results [7,9,12–14]. It was found to strongly limit pinching, leading to the fast electron beam maintaining a roughly constant radius [7,14]. This is consistent with the estimates above, as the numerical results are for average intensities greater than 10^{22} W m^{-2}. Signs of beam hollowing have been observed [7], again at an intensity consistent with the estimate for the generation of a positive magnetic field, but it was not examined in detail. The positive peak in the numerical results tends to be very sharp and concentrated near the axis, unlike that of Fig. 4. This is most likely due to the initial pinching, which produces a sharp current peak on axis, and to the fact that the resistivities used only decrease faster than linearly with temperature at high temperatures.

The change in magnetic field generation could explain a number of experimental results. Clark *et al.* [16] report the formation of an annular plasma on the back of targets (the side facing away from the laser) at intensities reaching 10^{24} W m^{-2}, whereas at intensities of 10^{23} W m^{-2} a narrow jet of plasma was observed [17]. This can be explained by beam pinching at the lower intensity [7], giving way to beam hollowing at the higher intensity. The intensities are again in line with the above estimates. However, Eq. (24) varies strongly with the absorption, which is not well known in the experiments. It is also possible that this is due to the electric field reducing the penetration of the beam front on axis, as discussed above. However, this would be a transitory effect, so appears to be a less likely explanation. Clark *et al.* [16] also report that the proton rings that they observed at a lower intensity [13] were replaced by disks. In the previous experiment, the protons were emitted from the back at specific angles determined by their energy, the lower the energy the larger the angle, forming rings on the detector. This was explained by protons passing through the target being deflected by the negative magnetic field generated by a fast electron beam. The disappearance of the rings for higher intensities is also consistent with the eventual fall and reversal of the magnetic field due to target heating. Differences in heating regimes could explain the apparent differences between the earlier results of Clark *et al.* [13] and those of Snavely *et al.* [18]. The annular peak in target heating reported by Koch *et al.* [19] does not appear to be directly explicable in terms of this result, due to its large radius. The expansion of the region of positive magnetic field, which can be seen in Fig. 4, is too slow to reach such a large radius during the laser pulse, and numerical results have always given a much smaller region of positive magnetic field.

The consequences of the eventual fall in the electric field with current density have been considered, for the Spitzer resistivity, by a number of authors. Our results show that these considerations apply whenever the resistivity falls faster than linearly with temperature. Haines [20] noted that the fall in the electric field would allow a larger current to flow, increasing the heating and thus further reducing the electric field, leading to an instability that he called the electrothermal instability. However, when the magnetic field becomes important the fast electrons are pushed away from regions of low resistivity, and it is the conduction current that increases, not the fast electron current. Batani *et al.* [5] considered the scaling of the electric field and the penetration depth of Eq. (2) with target density. This enters our equations via the heat capacity term C [Eq. (9)], and we obtain the same result as they did: the electric field scales as $E \propto n_b^{3/5}$ [Eq. (20)], therefore the penetration depth should scale as $L \propto n_b^{-3/5}$ [Eq. (2)]. They found this to be consistent with their experimental results on fast electron propagation through foams of different densities, which indicated $L \propto n_b^{-0.5}$. Applying Eq. (24) to their parameters indicates that the electric field should start to fall for the highest density used, that the magnetic field should start to change sign for the intermediate density used, and that the strong heating effects will clearly dominate the results for the lowest density used. Therefore a slower change in the penetration depth with density than predicted by the strong heating results might be expected. The effect of the magnetic field on the penetration depth is complicated. In general, it reduces penetration [12], thus as the magnetic field starts to fall the penetration could increase, but once a positive magnetic field starts to be generated it would start to fall again. Glinsky [6] considered the scaling of the penetration depth with time. For later times he obtained a $t^{3/5}$ scaling, as would be expected from Eq. (25).

Finally, we will use the results to estimate the beam parameters required for fast ignition by Ohmic heating, for which the rigid beam model is perfectly adequate. The goal here is to heat a hydrogen plasma with an electron number density of the order of 10^{32} m^{-3} from a temperature (kT/e) of a few eV to around 10 keV in a time not greater than around 10 ps [1]. From these parameters Eq. (8) can be used to determine the minimum current density required. As the physical significance of the current density is not clear, we use the fact that the velocity of the fast electrons cannot exceed that of light to give a lower limit on the electron density from $n > -j/ec$. As the final temperature is much greater than the initial value, we neglect this to give

$$n > \frac{1}{ec}\sqrt{\frac{CT}{(1-\alpha)\eta\tau}}, \quad \alpha < 1. \tag{27}$$

Using the Spitzer resistivity with a $Z \ln \Lambda$ of 10 and the heat capacity of an ideal gas at constant volume, approximations that should at least be valid as the temperature approaches the desired value, gives a minimum fast electron density of 6.46×10^{28} m^{-3}. The fast electrons must be generated with a density lower than that of the plasma where the laser is absorbed. This will be at most the critical density, which is $\approx 10^{15}\gamma/\lambda^2$ m^{-3}, where γ is the Lorentz factor of the electrons in the laser field. We thus require this to be much greater than the density given by Eq. (27). For nonrelativistic intensities this requires the wavelength to be much less than 0.124 μm, which is not, currently, practical. For a more realistic wavelength of 1 μm it requires the intensity to be much greater than 5.74×10^{25} W m^{-2}. If we take into account that the radius of the heated region must be at least 10 μm [1], then from this lower limit on the intensity combined with the pulse duration of 10 ps we see that the laser energy must be much greater than 180 kJ. At these strongly relativistic intensities the critical density varies as $1/\lambda$, so we can only gain a factor of 2 or 3 for realistic reductions in the laser wavelength. It should be pointed out that in determining these limits the only assumption we have made about the fast electron generation is that it occurs at a density less than the critical density. They are independent of factors such as the mean energy and the absorption. If we were to calculate the fast electron current density as we did in deriving Eq. (24) we would find that higher intensities and laser energies and lower wavelengths are required, even for high absorptions. Possible variations in the parameters used may lower these limits, but not by much more than an order of magnitude. The density of the fast electrons can be significantly increased by magnetic pinching. However, the magnetic field increases the curvature of the electrons' trajectories, lowering the forward velocity, and thus increasing the required density, so the gain is not as great as might be expected. More importantly, for fast ignition we must rapidly enter the strong heating regime, so, for the Spitzer resistivity, the magnetic field will largely act to expand the beam. The magnetic field could be of indirect benefit in that it will inhibit lateral heat flow, possibly relaxing the ignition requirements, but this is beyond the scope of this paper. A possibility that could greatly lower these limits is the presence of anomalous resistivity [2]. Whatever the process involved, we do not expect the mean free path of the background electrons to be reduced much below the mean interparticle separation. The magnetic field required to give a Larmor radius less than this is already greater than 10^5 T at an electron energy of 1 eV, which is not achievable in these circumstances. Taking the interparticle separation to be $n_b^{-1/3}$ gives

$$\eta \sim \frac{\sqrt{mkT}}{n_b^{2/3}e^2}, \tag{28}$$

where m is the electron mass. Using Eq. (28) gives a lower limit on the density of 5.49×10^{27} m^{-3}, which for a wavelength of 1 μm requires an intensity much greater than 4.02×10^{23} W m^{-2} and a laser energy much greater than 1.26 kJ. The difference is not as great as might be expected because for $kT/e < 380$ eV the Spitzer resistivity is higher than that of Eq. (28). Only in this extreme case does the scheme appear to be feasible, which was the conclusion reached by previous calculations on electron beam fusion [2]. The very much higher electron currents that can be generated by lasers do not significantly improve the situation. However, for the resistivity given by Eq. (28), the magnetic field would rapidly increase to the point where it turns the electrons back, and the current entering the target would be greatly reduced. This may not be a disadvantage, as Hain and Mulser [21] have shown that ignition can be triggered by heating the corona. Apart from this possibility, which relies on a somewhat unrealistic reisitivity, fast ignition by Ohmic heating from laser generated fast electrons does not appear to be feasible. The original fast ignitor proposal [1] relied on collisional energy deposition. This exceeds Ohmic heating if the fast electron energy is low enough. Electron energies of 0.5–1 MeV were considered to be ideal [1]. The constraint then is maintaining $I\lambda^2$ low enough while delivering sufficient energy in a short enough time. There is also a comparable lower limit on the fast electron density in this case, as calculated by Zepf *et al.* [22], which cannot be overcome by relativistic effects. These problems could be overcome by using many beams, possibly irradiating the whole spherical surface, thus maximizing the spot size and increasing the fast electron density by spherical convergence. This is almost a return to the classical configuration, but using a heat wave instead of a shock wave.

IV. CONCLUSIONS

We have solved the equations for the electric and magnetic fields generated by a rigid fast electron beam propagating in a conductor, including Ohmic heating and a resistivity with an arbitrary power law dependence on temperature. These results provide a qualitative assessment of the effect of temperature dependent resistivity on fast electron propagation in more realistic circumstances. We have seen that they can help to explain a number of numerical and experimental results on laser-generated fast electron transport in solid targets, and we have used them to give estimates for the fast ignitor scheme. It was shown that the fast electron density required to achieve ignition via Ohmic heating is unrealistically high.

[1] M. Tabak, J.M. Hammer, M.E. Glinsky, W.L. Kruer, S.C. Wilks, and J. Woodworth, Phys. Plasmas **1**, 1626 (1994).

[2] R.B. Miller, *An Introduction to the Physics of Intense Charged Particle Beams* (Plenum Press, New York, 1982), Chap. 4.

[3] A.R. Bell, J.R. Davies, S. Guerin, and H. Ruhl, Plasma Phys. Controlled Fusion **39**, 653 (1997).

[4] J.R. Davies, Laser Part. Beams **20**, 243 (2002).

[5] D. Batani, A. Antonicci, F. Pisani, T.A. Hall, D. Scott, F. Amiranoff, M. Koenig, L. Gremillet, S. Baton, E. Martinolli, C. Rousseaux, and W. Nazarov, Phys. Rev. E **65**, 066409 (2002).

[6] M.E. Glinsky, Phys. Plasmas **2**, 2796 (1995).

[7] J.R. Davies, A.R. Bell, and M. Tatarakis, Phys. Rev. E **59**, 6032 (1999).

[8] H.M. Milchberg, R.R. Freeman, S.C. Davey, and R.M. More, Phys. Rev. Lett. **61**, 2364 (1988).

[9] J.R. Davies, A.R. Bell, M.G. Haines, and S.M. Guerin, Phys. Rev. E **56**, 7193 (1997).

[10] A.R. Bell, J.R. Davies, and S.M. Guerin, Phys. Rev. E **58**, 2471 (1998).

[11] E.E. Fill, Phys. Plasmas **8**, 1441 (2001).

[12] J.R. Davies, Phys. Rev. E **65**, 026407 (2002).

[13] E.L. Clark, K. Krushelnick, J.R. Davies, M. Zepf, M. Tatarakis, F.N. Beg, A. Machacek, P.A. Norreys, M.I.K. Santala, I. Watts, and A.E. Dangor, Phys. Rev. Lett. **84**, 670 (2000).

[14] M. Borghesi, A.J. MacKinnon, A.R. Bell, G. Malka, C. Vickers, O. Willi, J.R. Davies, A. Pukhov, and J. Meyer-ter-Vehn, Phys. Rev. Lett. **83**, 4309 (1999).

[15] L. Gremillet, G. Bonnaud, and F. Amiranoff, Phys. Plasmas **9**, 941 (2002).

[16] E.L. Clark, M. Zepf, F.N. Beg, M. Tatarakis, C. Escoda, M. Norrefeldt, A.E. Dangor, K. Krushelnick, R.J. Clarke, P.A. Norreys, I. Spencer, and K.W.D. Ledingham, Central Laser Facility RAL Annual Report 1999-2000 (CLRC, 2000, http://www.clf.rl.ac.uk)

[17] M. Tatarakis, J.R. Davies, P. Lee, P.A. Norreys, N.G. Kassapakis, F.N. Beg, A.R. Bell, M.G. Haines, and A.E. Dangor, Phys. Rev. Lett. **81**, 999 (1998).

[18] R.A. Snavely, M.H. Key, S.P. Hatchett, T.E. Cowan, M. Roth, T.W. Phillips, M.A. Stoyer, E.A. Henry, T.C. Sangster, M.S. Singh, S.C. Wilks, A. MacKinnon, A. Offenberger, D.M. Pennington, K. Yasuike, A.B. Langdon, B.F. Lasinski, J. Johnson, M.D. Perry, and E.M. Campbell, Phys. Rev. Lett. **85**, 2945 (2000).

[19] J.A. Koch, M.H. Key, R.R. Freeman, S.P. Hatchett, R.W. Lee, D. Pennington, R.B. Stephens, and M. Tabak, Phys. Rev. E **65**, 016410 (2001).

[20] M.G. Haines, Phys. Rev. Lett. **47**, 917 (1981); M.G. Haines and F. Marsh, J. Plasma Phys. **27**, 427 (1982).

[21] S. Hain and P. Mulser, Phys. Rev. Lett. **86**, 1015 (2001).

[22] M. Zepf, E.L. Clark, K. Krushelnick, F.N. Beg, C. Escoda, A.E. Dangor, M.I.K. Santala, M. Tatarakis, I.F. Watts, P.A. Norreys, R.J. Clarke, J.R. Davies, M.A. Sinclair, R.D. Edwards, T.J. Goldsack, I. Spencer, and K.W.D. Ledingham, Phys. Plasmas **8**, 2323 (2001).